

A Theoretical Study of the Scavenging of O_2^- by NO in the Gas Phase and in Condensed Media

S. J. Knak Jensen,^{*,†} P. Mátyus,[‡] M. A. McAllister,[§] and I. G. Csizmadia^{||}

Department of Chemistry, Langelandsgade 140, Aarhus University, DK-8000 Aarhus C, Denmark, Semmelweis University of Medicine, Institute of Organic Chemistry, H-1092 Budapest, Högyes E. u. 7, Hungary, Department of Chemistry, P.O. Box 5068, University of North Texas, Denton, Texas 76203, and Lash Miller Chemical Laboratories, 80 St. George Street, University of Toronto, Toronto, Ontario M5S 3H6, Canada

Received: April 16, 2001; In Final Form: July 12, 2001

A mechanism describing the scavenging of O_2^- by NO to produce NO_3^- in the condensed phase is presented. In the proposed mechanism, H_2O acts as an overall catalyst. However, it is oxidized temporarily by $ONOO^-$ to a second intermediate complex consisting of NO_2^- and H_2O_2 . This complex is subsequently rearranged to hydrated nitrate, $[NO_3^-, H_2O]$. The structures of the various species in the elementary reactions are investigated by ab initio methods. The thermodynamical data in condensed media are estimated from polarized continuum calculations. Thermodynamic considerations show that the proposed mechanism is feasible. However, the estimates for the activation energies suggest that the mechanism is not of much physiological importance.

1. Introduction

In the oxidative stress, the cells are exposed to excessive levels of molecular oxygen or reactive oxygen species, like O_2^- . It is currently widely accepted that increases in oxidative stress are involved in a variety of diseases such as diabetes¹, atherosclerosis, and essential hypertension.^{2,3} Endothelium-derived nitric oxide plays an important role in the regulation of vascular tone via stimulation of vascular smooth muscle relaxation, and it also exhibits a number of beneficial effects on conditions associated with oxidative stress. Recently, it has been demonstrated that nitric oxide also plays a crucial role in the central nervous system: it is involved in neuromodulation, neurotransmission, and synaptic plasticity. A body of accumulating data, on the other hand, indicates that nitric oxide could act as an antioxidant as well as a prooxidant.⁴ Therefore, understanding the mechanism of interaction of nitric oxide with reactive oxygen species may lead to more successful and safer medical interventions of various pathophysiological processes involving oxidative stress. To shed some light on the basal chemical reactions involved, we have investigated theoretically a pathway for scavenging of O_2^- by nitric oxide to produce NO_3^- eventually.

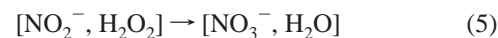
Previously, the formation of the peroxyxynitrite ion, $ONOO^-$, has been investigated in the gas phase, where the rate constants for the reactions



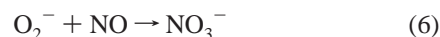
were measured by a flowing afterglow technique.⁵ The formation of $ONOO^-$ has also been studied in aqueous solution.^{6,7} The ion is stable in basic solutions for days, whereas at neutral pH,

its corresponding acid, peroxyxynitrous acid, ($pK_a = 6.8$), has a lifetime of a few seconds only.^{8,9} The reactivity of $ONOO^-$ is subject of much current research.^{10–12}

We consider the following mechanism for scavenging of O_2^- to harmless species in a water-containing medium:



with the overall process



Our investigation proceeds according to the following strategy. First, we use ab initio quantum chemical methods to estimate the enthalpy change for reaction 6 at various levels of theory for the purpose of assessing the accuracy of the methods by comparing to gas-phase thermodynamic data. As a result of this comparison, we establish the level of theory to be used in the investigation. Second, the structure and thermodynamics of the complexes, $ONOO^-$, formed by O_2^- and NO, are identified. Third, we investigate the reaction of $ONOO^-$ with one H_2O molecule to form a solvated complex $[ONOO^-, H_2O]$. This part encompasses an investigation of the structure and thermodynamics of the isomers $[NO_2^-, H_2O_2]$ and $[NO_3^-, H_2O]$. To study the trend in thermodynamics on solvation, we calculate structures and energies of $[ONOO^-, H_2O]$, $[NO_2^-, H_2O_2]$, and $[NO_3^-, H_2O]$ solvated by one water molecule. It is currently computationally unfeasible to follow the solvation process by adding more and more water molecules to small complexes. Instead, we use the approximate Tomasi method of polarized continuum simulations^{13,14} to estimate the thermodynamic

* Corresponding author. Phone: +(45)8942 3862. Fax: +(45)8619 6199. E-mail: kemskj@kemi.aau.dk.

† Aarhus University, Denmark.

‡ Semmelweis University of Medicine, Hungary.

§ University of North Texas, U.S.A.

|| University of Toronto, Canada.

TABLE 1: Standard Enthalpy Change ΔH° (kJ/mol) at 25 °C for Reaction 6 in the Gas Phase Calculated at Various Levels of Theory

MP2/ 6-31+G(d,p)	MP2/ AUG-cc-pVDZ	B3LYP/ 6-31+G(d,p)	experimental
-382.4	-388.5	-345.9	-350.9

properties of the species in condensed media. That is, we find the energies of the various species in a medium with a chosen dielectric constant. Finally, we calculate the transition states and activation energies pertaining to the reaction mechanism (eqs 4 and 5) in the gas phase and subsequently in aqueous solution.

The article is organized as follows: In section 2, we list the used theoretical methodologies, and we compare the calculated enthalpy changes for the overall reaction 6 to thermodynamical data. In section 3, we present the structures of the various reactants, intermediates, and products, and we list the enthalpy changes for reactions 2–5. Section 4 contains the results from the polarized continuum simulations, and section 5 deals with the transition states and activation energies. Finally, the results are discussed and summarized in section 6.

2. Computational Details

The structures of the various species appearing in eqs 2–6 were determined by quantum chemical *ab initio* optimizations using the package Gaussian98.¹⁵ The chosen levels of theory were second-order Möller–Plesset (MP2) and a hybrid DFT (B3LYP) method. In a special case, the coupled cluster method (CCSD) was used to decide among conflicting results. No geometry constraints were used in the optimizations. The determination of transition states was facilitated by using a synchronous transit-guided quasi-Newton method.¹⁶ Explicit calculations (IRC) were performed to identify the structures linked by the transition states. We used the basis sets 6-31+G(d,p)¹⁷ and AUG-cc-pVDZ.¹⁸ The standard enthalpy change, ΔH° , for the overall reaction 6 was calculated at the various levels of theory. The results are listed in Table 1, which shows that the best agreement with thermodynamic data is obtained with the B3LYP/6-31+G(d,p) method.

The identification of hydrogen bonds in the various complexes is based on distances. Whenever the distance between a hydrogen atom (in H_2O or H_2O_2) and an electronegative atom in another molecule or ion is less than the threshold distance given by the sum of the van der Waals radii of the involved atoms, we may assign a hydrogen bond between them.

3. Ab Initio Results

3.1. Complexes between O_2^- and NO. Both O_2^- and NO have electronic ground states that are spin doublets. The binary complexes formed from them are therefore either spin singlets or spin triplets. The calculations show that the singlet and triplet complexes are similar in structure. The electronic energy of the triplet states, however, is about 80 kJ/mol higher than that of the singlets (at the MP2 level of theory), and consequently, the triplet complexes will not be considered any further.

Two conformers of the complex formed by O_2^- and NO are shown in Figure 1 along with the nitrate ion isomer and the separated doublets. It appears from Figure 1 that the cis conformer has an electronic energy 13 kJ/mol lower than that of the trans isomer. This number agrees well with the result of calculations performed at a higher level of theory.²¹ Both conformers are planar. Actually, an additional complex between O_2^- and NO was identified at the MP2/AUG-cc-pVDZ level. This complex was pyramidal-like and could be considered as

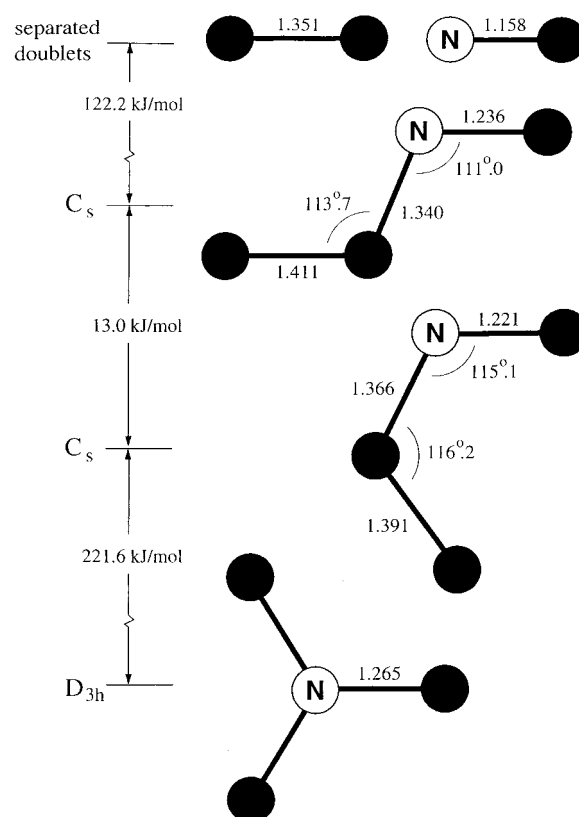


Figure 1. Structures of O_2^- and NO and their complexes calculated at the B3LYP/6-31+G(d,p) level of theory. The numbers indicate the difference in electronic energy between the structures connected by the arrow. The distances and angles are in Å and deg, respectively. The experimental value of the internuclear distances in O_2^- and NO are 1.347 ± 0.005 ¹⁹ and 1.1506 Å,²⁰ respectively. In this and all subsequent figures, ● indicates an oxygen atom, and ○ indicates a hydrogen atom.

an insertion of the N atom between the atoms of O_2^- . At the B3LYP/6-31+G(d,p) level, this complex turned into the trans conformer of ONOO^- . To resolve the conflicting results from these two methods, we optimized the pyramidal structure using the advanced theory of coupled cluster CCSD/6-31+G(d,p). It turned out that the MP2/AUG-cc-pVDZ structure collapsed into the trans conformer, indicating that the pyramidal structure is likely to be fictitious in the ground state whereas it may actually be the transition state in the photochemical conversion of NO_3^- to ONOO^- .

3.2. [ONOO⁻, H₂O] and [OONO⁻, 2H₂O] Complexes. Several structurally different complexes result when the peroxy nitrite ion is solvated by a single water molecule, [ONOO⁻, H₂O]. It appears from the calculations that a water molecule tends to solvate at the terminal positions in ONOO⁻. Also, it is energetically more attractive for a water molecule to bind to the OO part of ONOO⁻ than to the NO part. In Figure 2, we show four of the complexes. There are additional conformers, separated in energy by a few kilojoules per mole only. The complexes B, C, and D are planar. The hydrate with the lowest energy has a cis configuration of the ONOO⁻ moiety.

The complexes [ONOO⁻, H₂O] are isomeric with the complex, [NO₂⁻, H₂O₂], which may be formed from NO₂⁻ and H₂O₂. It is also isomeric with the complex formed by solvating a NO₃⁻ ion with one water molecule. (A complex formed from H₂OO and NO₂⁻ was also identified. The energy of this complex is 30.7 kJ/mol higher than the energy sum of the separated species ONOO⁻ and H₂O and will therefore not be considered any further.) In Figure 3, we display the three types of isomers.

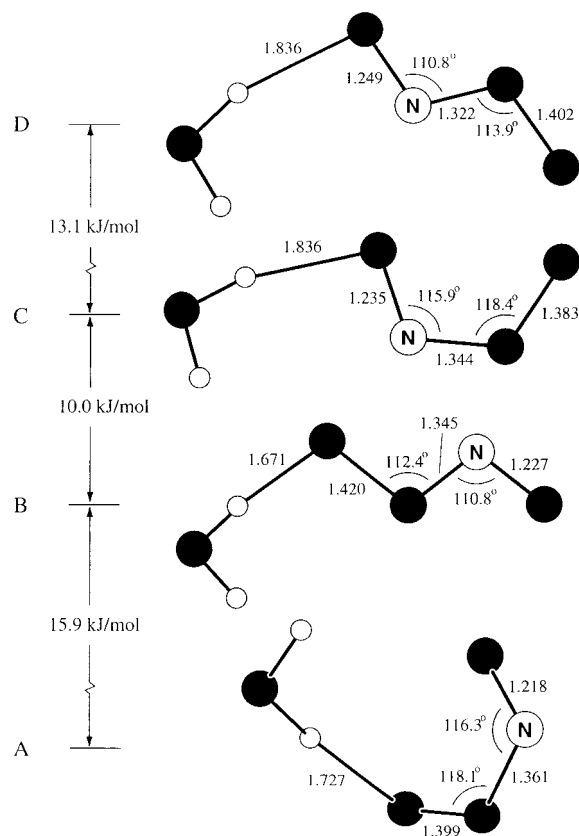
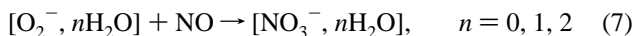


Figure 2. Structures of complexes, $[ONOO^-, H_2O]$, formed from the *cis* and *trans* conformers of the peroxyntirite ion, $ONOO^-$, and a water molecule. The structures are calculated at the B3LYP/6-31+G(d,p) level of theory. The symbols are explained in Figure 1.

For future reference, Figure 3 also includes three isomers (A, B, and C) of $[NO_2^-, H_2O_2]$, which differ in the orientation of the hydrogen bonds. It appears that the $[ONOO^-, H_2O]$ and $[NO_2^-, H_2O_2]$ complexes are rather close in energy, whereas the energy separation between $[NO_2^-, H_2O_2]$ and $[NO_3^-, H_2O]$ is substantially larger. In Figure 4, we show some selected complexes of the three types of isomers with one additional water molecule.

4. Results from Polarized Continuum Simulations

Before we describe the effect of solvation in a medium with dielectric constant, ϵ , we will consider the overall reaction 6 in aqueous solution because available experimental data offers a benchmark in this case. Thus, we study the reaction



where we have chosen to place all n water molecules on O_2^- and none on NO because the solvation enthalpy for O_2^- is about 1 order of magnitude larger than that for NO. From the *ab initio* results, we may derive $\Delta H^\circ(n)$ at 25 °C. We may also calculate the energy change, $\Delta E(n)$, for the reaction in a solvent with the dielectric constant of water using the polarized continuum method. $\Delta H^\circ(n)$ and $\Delta E(n)$ are listed in Table 2 along with the experimental standard enthalpy change for the reaction in water, $\Delta H^\circ(aq)$. It appears that $\Delta H^\circ(n)$ rises (from larger negative toward smaller negative values) with n and that $\Delta H^\circ(n=2)$ is roughly midway between the experimental values in the gas phase and the aqueous solution. $\Delta E(n)$ also increases with n , and $\Delta E(n=2)$ is very close to the experimental value $\Delta H^\circ(aq)$, suggesting that the polarized continuum approximation will give

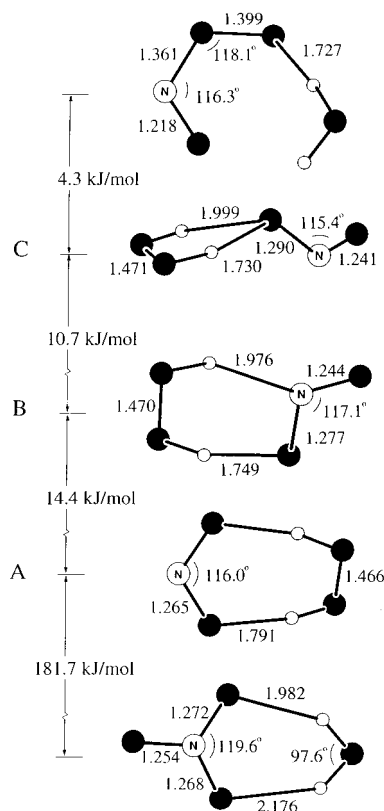


Figure 3. Structures of selected isomers, $[ONOO^-, H_2O]$, $[NO_2^-, H_2O_2]$, and $[NO_3^-, H_2O]$, calculated at the B3LYP/6-31+G(d,p) level of theory. The symbols are explained in Figure 1.

a good description of the thermodynamics of this system. In Figure 5, we show $\Delta E(n)$ as a function of ϵ . We note that small values of the dielectric constants model a hydrophobic environment, such as a cell membrane, whereas large ϵ values are representative of a hydrophilic environment. As might be expected, $\Delta E(n)$ exhibits a steep rate of change for small values of ϵ (≤ 5) and a modest, almost linear, growth for larger values.

5. Transition States

$n = 0$ Case. We have found that the reaction *cis*- $ONOO^- \rightarrow NO_3^-$ proceeds through two transition states. The first one is a *cis*-*trans* rearrangement. At the B3LYP/6-31+G(d,p) level of theory, the activation energy for this process is 113 kJ/mol, which is in good agreement with the values 88–100 kJ/mol obtained by Tsai et al.²² using higher levels of theory. The other transition state connects *trans*- $ONOO^-$ with NO_3^- . The energy of this state is 208 kJ/mol higher than the energy of *trans*- $ONOO^-$. The large value of the activation energy is consistent with the absence of NO_3^- in the gas-phase reaction of O_2^- and NO.⁵ The activation energies are found to be the same within 1–2% in a medium corresponding to water.

$n = 1$ Case. We have investigated two reaction paths leading from *cis*- $[ONOO^-, H_2O]$ to $[NO_3^-, H_2O]$. The first one is the direct transition between the two species. It appears that the transition proceeds through the *trans* isomer. The transition state is depicted in Figure 6. The activation energies from the *trans*- $[ONOO^-, H_2O]$ isomer are 214 and 216 kJ/mol in the gas and aqueous phases, respectively.

The other reaction path follows the mechanism described in eqs 3–5. The calculations show this path involves four transition states, which are depicted in Figure 7. In passing, we note that the long O–O bonds found in the transition states I and IV are similar to the long O–O bond in the transition state connecting

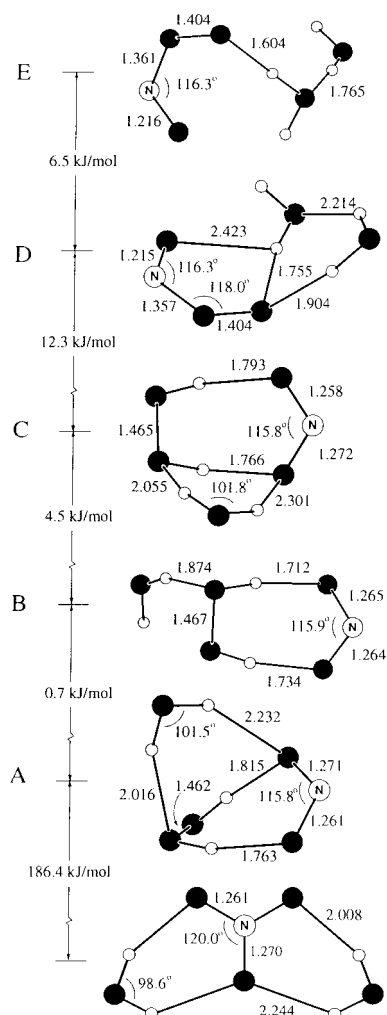


Figure 4. Structures of selected isomers, $[\text{ONOO}^-, 2\text{H}_2\text{O}]$, $[\text{NO}_2^-, \text{H}_2\text{O}_2, \text{H}_2\text{O}]$, and $[\text{NO}_3^-, 2\text{H}_2\text{O}]$, calculated at the B3LYP/6-31+G(d,p) level of theory. The symbols are explained in Figure 1.

TABLE 2: Some Data (kJ/mol) for the Reaction $[\text{O}_2^-, n\text{H}_2\text{O}] + \text{NO} \rightarrow [\text{NO}_3^-, n\text{H}_2\text{O}]$ ($n = 0, 1, 2$)^a

n	$\Delta H^\circ(n)$	$\Delta E(n)$
0	-345.9	-295.3
1	-317.2	-284.2
2	-298.3	-271.1

^a $\Delta H^\circ(n)$ is the standard enthalpy change at 25 °C calculated at the B3LYP/6-31+G(d,p) level of theory. $\Delta E(n)$ is the energy change in a continuum with the dielectric constant of water calculated at the B3LYP/6-31+G(d,p) level of theory using the polarized continuum approximation. The experimental standard enthalpy change ΔH° at 25 °C for the reaction $\text{O}_2^-(\text{aq}) + \text{NO}(\text{g}) \rightarrow \text{NO}_3^-(\text{aq})$ is -264.3 ± 8 kJ/mol.

peroxynitrous acid and nitric acid.²³ The transition state with the highest energy is the one that connects *cis*- $[\text{ONOO}^-, \text{H}_2\text{O}]$ and $[\text{NO}_2^-, \text{H}_2\text{O}_2]$. In the gas phase, the activation energy is 139 kJ/mol, and in aqueous solution, it is 120 kJ/mol. The variation of the energies along the reaction path is shown in Figure 8.

$n = 2$ Case. In this case, we have only investigated the second reaction path and only the transition which involves the largest activation energy in the case of $n = 1$, i.e., the reaction *cis*- $[\text{ONOO}^-, 2\text{H}_2\text{O}] \rightarrow [\text{NO}_2^-, \text{H}_2\text{O}_2, \text{H}_2\text{O}]$. Experience gained from other studies²⁴ suggests that the extra water molecule may increase the flexibility of the transition state, which may lead to a reduction of the activation energy. The transition state is depicted in Figure 9. The calculation shows that the activation

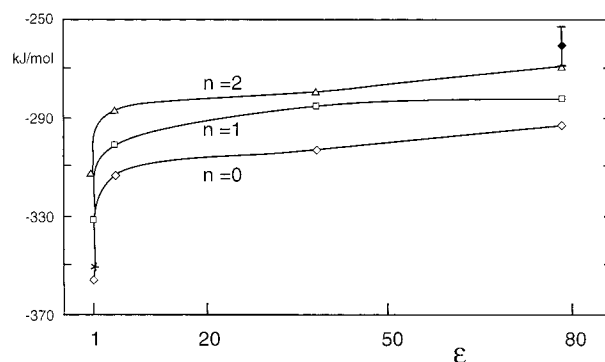


Figure 5. Change in energy for the reaction $[\text{O}_2^-, n\text{H}_2\text{O}] + \text{NO} \rightarrow [\text{NO}_3^-, n\text{H}_2\text{O}]$, $n = 0, 1, 2$, as a function of the dielectric constant, ϵ , of the solvent. The data are calculated at the B3LYP/6-31+G(d,p) level of theory, and the solvation energy is derived from the Tomassi continuum model. * and \blacklozenge indicate the experimental values for standard enthalpy change ΔH° at 25 °C in the gas and aqueous phases, respectively.

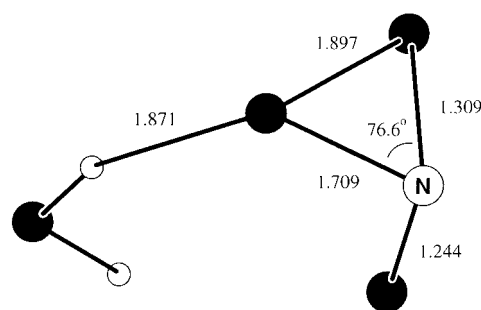


Figure 6. Transition state connecting *trans*- $[\text{ONOO}^-, \text{H}_2\text{O}]$ (B in Figure 2) with the $[\text{NO}_3^-, \text{H}_2\text{O}]$ complex. The structure is determined at the B3LYP/6-31+G(d,p) level of theory.

energies are 135 and 127 kJ/mol in the gas and aqueous phases, respectively. These values are very close to the values obtained in the case of $n = 1$, which is in line with the similarity of the two transition states in Figure 9 and Figure 7 (I). Consequently, the evidence derived from the $n = 1$ and $n = 2$ cases suggests that the activation energy is too high for the reaction mechanism to be of much physiological importance.

6. Discussion and Summary

The calculations have shown that the activation energy for the direct ONOO^- to NO_3^- reaction is high—in excess of 200 kJ/mol. The proposed stepwise mechanism 3–5, where water acts as a catalyst, requires substantially lower activation energy to proceed. The highest activation energies are 139 and 127 kJ/mol in the gas and aqueous phases, respectively. However, the value in the aqueous phase is too high for the mechanism to be of much physiological importance. This conclusion is in accordance with the experimental observation that the peroxynitrite ion is stable for days in basic solution. Another merit of the mechanism is that it seems to offer an easy explanation for the presence of NO_2^- and H_2O_2 in aqueous solutions of NO_3^- that have been exposed to UV radiation.²¹

The above estimates for the activation energies were obtained using the approximate theory of B3LYP/6-31+G(d,p). It is pertinent to consider if a more advanced theoretical method may change our findings qualitatively. This question may be answered by comparing our data for the activation energy for the *cis*- $\text{ONOO}^- \rightarrow \text{trans-ONOO}^-$ reaction to data derived from higher levels of theory. Our estimate is 113 kJ/mol, whereas other investigators find 88–100 kJ/mol, which amounts to a

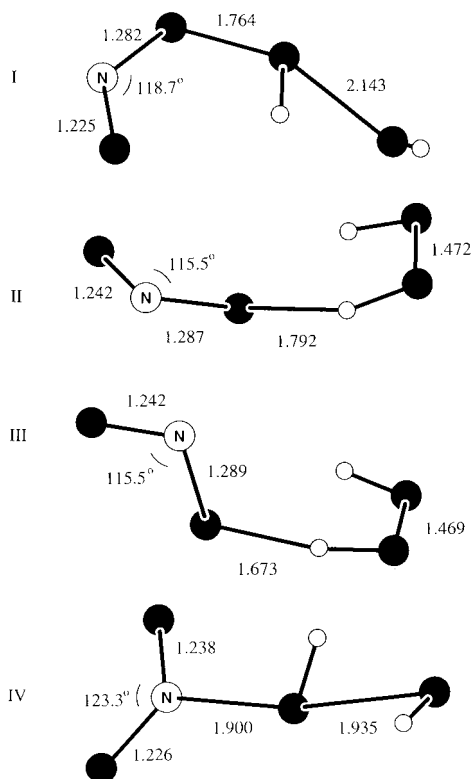


Figure 7. Four transition states determined at the B3LYP/6-31+G(d,p) level of theory. I connects *cis*-[ONOO⁻, H₂O] (A in Figure 2) with [NO₂⁻, H₂O₂] (A in Figure 3). II connects the A and C isomers of [NO₂⁻, H₂O₂] in Figure 3. III connects the C and B isomers of [NO₂⁻, H₂O₂] in Figure 3. IV connects the B isomer of [NO₂⁻, H₂O₂] (Figure 3) with the [NO₃⁻, H₂O] complex.

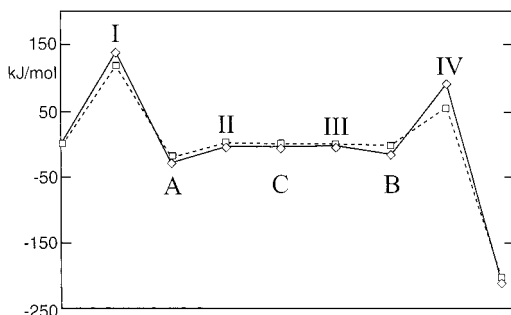


Figure 8. Sketch of a reaction path for the overall reaction *cis*-[ONOO⁻, H₂O] → [NO₃⁻, H₂O]. I–IV indicate the transition states shown in Figure 7 and A–C refer to the complexes depicted in Figure 3. Thus, I and IV are associated with reactions 4 and 5, respectively, while II and III correspond to rearrangements of the [NO₂⁻, H₂O₂] complex. The full line connects the gas-phase data, and the dashed line connects the data for the aqueous solution. The energies are relative to the energy of *cis*-[ONOO⁻, H₂O].

reduction of 12–22%. If this reduction can be carried over to the hydrated species, then the lowest estimate for the activation energy for the reaction mechanism 3–5 will be 99 kJ/mol, which corresponds to a very slow reaction.

In addition, we have probed the sensitivity of the activation energies to the basis set by calculating the activation energy for the *cis*-[ONOO⁻, H₂O] → [NO₂⁻, H₂O₂] reaction using the

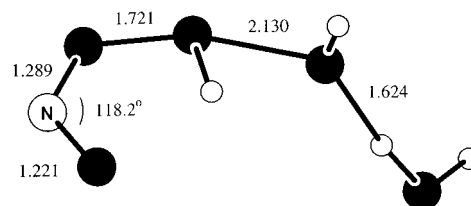


Figure 9. Structure of the transition state connecting *cis*-[ONOO⁻, 2H₂O] (E in Figure 4) with [NO₂⁻, H₂O₂, H₂O] (B in Figure 4). The transition state is determined at the B3LYP/6-31+G(d,p) level of theory.

basis set AUG-cc-pVDZ. In this case, we find that the activation energy is 136 kJ/mol, whereas the calculations at B3LYP/6-31+G(d,p) lead to 139 kJ/mol. This small reduction is of no significance for the conclusion.

References and Notes

- (1) Laight, D. W.; Carrier, M. J.; Ånggård, E. E. *Cardiovasc. Res.* **2000**, *47*, 457.
- (2) Carr, A.; Frei, B. *Free Radical Biol. Med.* **2000**, *28*, 1806.
- (3) Taddei, S.; Virdis, A.; Ghiadoni, L.; Salvetti, G.; Salvetti, A. J. *Nephrol.* **2000**, *13*, 205.
- (4) Saugstad, O. D. *Acta Paediatr.* **2000**, *89*, 905.
- (5) Fehsenfeld, C.; Ferguson, E. E. *J. Chem. Phys.* **1974**, *61*, 3181.
- (6) Huie, R. E.; Padjama, S. *Free Radical Res. Commun.* **1993**, *18*, 195.
- (7) Goldstein, S.; Czapski, G. *Free Radical Biol. Med.* **1995**, *19*, 505.
- (8) King, P. A.; Anderson, V. E.; Edwards, J. O.; Gustafson, G.; Plumb, R. C.; Suggs, J. W. *J. Am. Chem. Soc.* **1992**, *114*, 5430.
- (9) Koppenol, W. H.; Moreno, J. J.; Pryor, W. A.; Ischiropoulos, H.; Beckman, J. S. *Chem. Res. Toxicol.* **1992**, *5*, 834.
- (10) Lemerrier, J.-N.; Padmaja, S.; Cueto, R.; Squadrito, G. L.; Uppu, R. M.; Pryor, W. A. *Arch. Biochem. Biophys.* **1997**, *345*, 160.
- (11) Knudsen, F. S.; Penatti, C. A. A.; Royer, L. O.; Bidart, K. A.; Christoff, M.; Ouchi, D.; Bechara, E. J. H. *Chem. Res. Toxicol.* **2000**, *13*, 317.
- (12) Jourde'heuil, D.; Miranda, K. M.; Kim, S. M.; Espey, M. G.; Vodovotz, Y.; Laroux, S.; Mai, C. T.; Miles, A. M.; Grisham, M. B.; Wink, D. A. *Arch. Biochem. Biophys.* **1999**, *365*, 92.
- (13) Miertuș, S.; Tomasi J. *Chem. Phys.* **1982**, *65*, 239.
- (14) Miertuș, S.; Scrocco, E.; Tomasi, J. *Chem. Phys.* **1981**, *55*, 117.
- (15) Frisch, M. J.; Trucks, G. W.; Schlegel, H. B.; Scuseria, G. E.; Robb, M.; Cheeseman, J. R.; Zakrzewski, V. G.; Montgomery, Jr. J. A.; Stratmann, R. E.; Burant, J. C.; Dapprich, S.; Millam, J. M.; Daniels, A. D.; Kudin, K. N.; Strain, M. C.; Farkas, O.; Tomasi, J.; Barone, V.; Cossi, M.; Cammi, R.; Mennucci, B.; Pomelli, C.; Adamo, C.; Clifford, S.; Ochterski, J.; Petersson, G. A.; Ayala, P. Y.; Cui, Q.; Morokuma, K.; Malick, D. K.; Rabuck, A. D.; Raghavachari, K.; Foresman, J. B.; Cioslowski, J.; Ortiz, J. V.; Stefanov, B. B.; Liu, G.; Fox, D. J.; Keith, T.; Al-Laham, M. A.; Peng, C. Y.; Nanayakkara, A.; Gonzales, C.; Challacombe, M.; Gill, P. M. W.; Johnson, B.; Chen, W.; Wong, M. W.; Andres, J. L.; Head-Gordon, M.; Replogle, E. S.; Pople, J. A. *Gaussian 98*, Revision A.6; Gaussian, Inc.: Pittsburgh, PA, 1998.
- (16) Peng, C.; Ayala, P. Y.; Schlegel, H. B.; Frisch, M. J. *J. Comput. Chem.* **1996**, *17*, 49.
- (17) Hehre, W. J.; Radom, L.; von Schleyer, P.; Pople, J. A. *Ab Initio Molecular Orbital Theory*; Wiley: New York, 1986.
- (18) Dunning, T. H., Jr. *J. Chem. Phys.* **1989**, *90*, 1007.
- (19) Travers, M. J.; Cowles, D. C.; Ellison, G. B. *Chem. Phys. Lett.* **1989**, *164*, 449.
- (20) *CRC Handbook of Chemistry and Physics*, 73rd ed.; CRC Press: Boca Raton, FL, 1992.
- (21) Tsai, J.-H. M.; Harrison, J. G.; Martin, J. C.; Hamilton, T. P.; van der Woerd, M.; Jablonsky, M. J.; Beckman, J. S. *J. Am. Chem. Soc.* **1994**, *116*, 4115.
- (22) Tsai, H.-H.; Hamilton, T. P.; Tsai, J.-H. M.; v. d. Woerd, M.; Harrison, J. G.; Jablonsky, M. J.; Beckman, J. S.; Koppenol, W. H. *J. Phys. Chem.* **1996**, *100*, 15087.
- (23) Sumathi, R.; Peyerimhoff, S. D. *J. Chem. Phys.* **1997**, *107*, 1872.
- (24) Morokuma, K.; Muguruwa, C. *J. Am. Chem. Soc.* **1994**, *116*, 10316.